Vision Research 48 (2008) 2649–2656

Contents lists available at ScienceDirect

Vision Research

journal homepage: www.elsevier.com/locate/visres

Sequential processing in vision: The interaction of sensitivity regulation and temporal dynamics

Vivianne C. Smith [a], Joel Pokorny [a,*], Barry B. Lee [b,c], Dennis M. Dacey [d]

[a] The University of Chicago, Opthalmology and Visual Science, 940 East 57th Street, Chicago, IL 60637, USA
[b] State University of New York College of Optometry, NY, USA
[c] The Max Planck Institute for Biophysical Chemistry, Göttingen, Germany
[d] The University of Washington, Seattle, WA, USA

ARTICLE INFO

Article history:
Received 30 October 2007
Received in revised form 21 April 2008

Keywords:
Temporal contrast sensitivity
Horizontal cell
Ganglion cell
Primate
Psychophysics

ABSTRACT

The goal of this work was to describe the interaction of sensitivity regulation and temporal dynamics through the primate retina. A linear systems model was used to describe the temporal amplitude sensitivity at different retinal illuminances. Predictions for the primate H1 horizontal cell were taken as the starting point. The H1 model incorporated an early time-dependent stage of sensitivity regulation by the cones. It was adjusted to reduce the effects of gap junction input and then applied as input to a model describing temporal amplitude sensitivity of Parvocellular and Magnocellular pathway retinal ganglion cells. The ganglion cell model incorporated center–surround subtraction. The H1 based model required little modification to describe the Parvocellular data. The Magnocellular data required a further time-dependent stage of sensitivity regulation that resulted in Weber's Law. Psychophysical data reflect the sensitivity regulation of the retinal ganglion cell pathways but show a decline in temporal resolution that is most pronounced for the post-retinal processing of Parvocellular signals.

1. Introduction

Psychophysical temporal contrast sensitivity functions (TCSF) measured at a number of fixed illuminance levels have revealed two important properties of the human visual system: sensitivity regulation and the dynamic response of the system. Thresholds at very low frequencies demonstrate sensitivity regulation. For the dynamic response, with luminance modulation at low retinal illuminances (c. 1–5 td), the TCSF is low-pass with a high frequency cut-off near 20 Hz. At high retinal illuminances (c. 10,000 td), the TCSF is band-pass with maximal sensitivity near 10 Hz and a high frequency cut-off near 60 Hz. The actual shape of the TCSF depended on the spatial parameters. For example, a large edgeless stimulus field (Kelly, 1961) emphasized the band-pass characteristic more than a 2° foveal field in a surround (de Lange, 1954). Nonetheless the transition from low-pass, low frequency cut-off TCSF at low retinal illuminance to band-pass, high frequency cut-off TCSF at high retinal illuminance was still present. A second technique, also introduced by de Lange (1958) and Kelly (1974), used stimuli varying sinusoidally in chromaticity at a constant retinal illuminance (Swanson, Ueno, Smith, & Pokorny, 1987). These chromatic TCSFs also varied with retinal illuminance level but differed in two important ways from achromatic TCSFs. The chromatic functions were primarily low-pass and the high frequency cut-offs occurred at much lower frequencies at a matched retinal illuminance level.

The goal of the present paper was to ask how and where in the primate cone pathways luminance sensitivity regulation and temporal dynamics interact. In the outer retina, photoreceptors and bipolar cells communicate by graded electrotonic transmission and chemical synapses. In the inner retina, retinal ganglion cells receive graded signals from the bipolar cells and transmit impulses to the Lateral Geniculate Nucleus (LGN). In the primate retina the two most numerous classes of retinal ganglion cells are the midget cells transmitting signals to the parvocellular layers (PC-pathway) and the parasol cells transmitting signals to the magnocellular layers (MC-pathway) of the LGN. The midget cells transmit spectral information deriving from the subtraction of signals from the middle (MWS) and long (LWS) wavelength sensitive cones and show strong responses to chromatic modulation. The parasol cells receive additive input from the LWS and MWS cones and are very sensitive to achromatic modulation but also show evidence of cone-opponent input at low temporal frequencies (Smith, Lee, Pokorny, Martin, & Valberg, 1992).

The TCSF has been measured in the outer (Smith, Pokorny, Lee, & Dacey, 2001) and inner (Lee, Martin, & Valberg, 1989; Lee, Pokorny, Smith, Martin, & Valberg, 1990) retina, employing similar

* Corresponding author.
E-mail address: j-pokorny@uchicago.edu (J. Pokorny).

0042-6989/$ - see front matter © 2008 Elsevier Ltd. All rights reserved.
doi:10.1016/j.visres.2008.05.002

stimuli and data collection methodology. Intracellular recordings were made from the horizontal cells of primates (Dacey, Diller, Verweij, & Williams, 2000; Dacey, Lee, Stafford, Pokorny, & Smith, 1996) using an *in vitro* preparation. We assumed that the dynamics of the horizontal cell, at the first synapse from the photoreceptors, reflect the photoreceptor output (Smith et al., 2001). Extracellular recordings of retinal ganglion cells of primates have been made using an *in vivo* preparation (Lee et al.,1989, 1990). The stimuli presented in these physiological measurements were very similar to those used in the psychophysical studies of Swanson et al. (1987). In this paper we start with TCSF data from H1 cells that were fit by a linear system model (Smith et al., 2001). We then examined TCSF data from retinal ganglion cells (Lee et al., 1990). We asked what modifications of the H1 cell linear system model were required to fit the retinal ganglion cell data. In both studies, we avoided rod participation by preventing any dark adaptation of the retina.

The results showed that there is an early time-dependent stage of sensitivity regulation at the level of the cones, which remains in the PC-pathway virtually unaltered. The MC-pathway shows a further time-dependent stage of sensitivity regulation at the retinal ganglion cell level. This additional stage of sensitivity regulation results in Weber's Law for the MC-pathway. Finally, the sensitivity regulation is preserved in psychophysical thresholds but sensitivity at high temporal frequencies is reduced, suggesting that post-retinal mechanisms limit psychophysical threshold at high temporal frequencies, especially in the PC pathway.

2. Materials and methods

This analysis incorporates previously published data. Here we give a brief review of the preparations and methods used. The retinal illuminances are specified in human equivalent trolands, which can be calculated for both outer and inner retinal preparations.

2.1. Outer retina

Intracellular recordings were made from anatomically identified H1 type horizontal cells in an in vitro preparation of the macaque monkey retina (Dacey et al., 1996). Macaque H1 cells correspond to the common axon-bearing horizontal cell population of the mammalian retina (Boycott & Dowling, 1969; Boycott and Kolb, 1973). In primates, each H1 cell receives combined input from LWS and MWS cone types but avoids contact with S cones (Dacey et al., 1996; Goodchild, Chan, & Grunert, 1996). The H1 cell receptive field can be described as a sum of two exponentials (Packer & Dacey, 2002) deriving from a direct input through H1 dendrites extending to the cone pedicles, and an indirect input through gap junctions between H1 cells. The direct input forms the major source of the cell response in the light adapted retina. The size of the H1 receptive field scales with eccentricity but does not depend on retinal illuminance. There is rod input to the H1 cell consistent with rod-cone gap junctions. Prolonged dark adaptation is required to measure the rod response (Verweij, Peterson, Dacey, & Buck 1999). The *in vitro* retinal preparation included pigment epithelium and choroid and was placed in a superfusion chamber as described fully in Dacey et al. (1996). The chamber was positioned on the stage of a light microscope. A light emitting diode-based stimulator coupled to an optical system was used to project a 5° field onto the retinal surface via the microscope camera port. The data were collected using 554 nm and 638 nm LEDs, preset at equiluminance and modulated by temporal sinusoids. The approximate maximal retinal illuminance was estimated to be 1000 td based on the physical calibration and after compensation for the Stiles–Crawford effect. The calibration was consistent with a comparison with extracellular recordings of MC-pathway cells the *in vivo* preparation (Lee et al., 1989, 1990). The majority of cells were sampled at 10 mm from the fovea (about 50° in the periphery).

2.2. Inner retina

The data for the inner retina were taken from retinal ganglion cells (RGC) of macaque recorded extracellularly in vivo (Lee et al., 1990). Data were restricted to presumed LGN-projecting PC-pathway midget cells and MC-pathway parasol ganglion cells identified by standard criteria. The acute *in vivo* preparation was fully described in Lee et al. (1989). Electrodes inserted through the sclera and vitreous allowed extracellular recording of impulse activity. A multi-channel Maxwellian view using luminance matched 554 nm and 638 nm LEDs provided temporal sinusoidally modulated stimuli. The data were collected with a 4.7° stimulus field. The approximate maximal retinal illuminance was estimated to be 2000 td based on the physical calibration. The cells were sampled within 3–10° of the fovea. Although different retinal eccentricities were sampled in the *in vitro* and *in vivo* recordings, we assumed that foveal and peripheral regions would show similar temporal filters and sensitivity regulation although time constants might show minor variation (Solomon, Martin, White, Ruttiger, & Lee, 2002).

2.3. Stimuli and responses

For both preparations, responses were measured at a number of temporal frequencies of the sinusoidal waveform. At each frequency, responses were measured to a series of Michelson contrasts ranging from 0.0325 to 1.0. For the H1 cell, the LEDs were modulated in phase; for the RGC cells both in phase and counterphase modulation was used. The sinusoids were presented for approximately 5 s to allow averaging of multiple responses. Retinal illuminance was varied by insertion of calibrated neutral density filters.

The H1 cells gave a graded hyperpolarization to light. After penetration and settling, the H1 cell gave about a −10 mV response to a 100 td, 10 ms light pulse. With temporal modulation, the response amplitude followed the waveform with a phase delay and minimal waveform distortion at low contrasts. The data were first analyzed with fast Fourier Transforms (FFTs) to obtain first harmonic amplitude and phase. The amplitude increased linearly with Michelson contrast except at low frequencies (<1 Hz) and high contrast (>0.5), conditions that did show distortion. We fit the linear portions of the data and the slope gave a measure of contrast gain (mV/contrast). The phase was constant for all contrasts and we estimated phase from the 0.25 contrast condition.

RGCs showed a resting discharge of 20–40 impulses/second (imp/s) and increased their firing rate to the preferred contrast (increments for ON-cells and decrements for OFF-cells). With temporal sinusoids the ON- and OFF-cells differed only in response phase. The FFTs were obtained from the peristimulus time histograms to obtain first harmonic amplitude and phase. For PC-pathway cells the Fourier amplitude increased with Michelson contrast showing static saturation non-linearity; the phase was constant. For MC-pathways cells, the amplitude also followed a saturation non-linearity but there were phase advances with increasing contrast. For both cell types the amplitude data were fit with a Michaelis–Menten saturation equation ($R = R_{max}c/[c + C_{sat}]$), where R is the Fourier amplitude, c is Michelson contrast, R_{max} is the maximal response and C_{sat} is the contrast at which R is one half R_{max}. Contrast gain, also termed responsivity, was determined as the initial slope of this function (R_{max}/C_{sat}) in impulses per second per% contrast. The phase was estimated at the lowest contrast at which a reliable response was obtained (first harmonic amplitude of 10 imp/s).

For all cells, contrast sensitivity was re-expressed as amplitude responsivity by dividing amplitude by the average retinal illuminance. This operation spreads the functions on the vertical axis, so that the low frequency data can be distinguished more clearly.

2.4. Analysis

The amplitude and phase data were fit using a cascade of filters based on linear systems. These included first and second order filters and time delays (Milsum, 1966). Individual fits were made at each illuminance level. A first order cascade with a pure delay has been used previously to describe the rod and the cone light response from the cone a-wave of the human ERG (Hood & Birch, 1993; Lamb & Pugh, 1992). Recently van Hateren (2005, 2007) proposed a more detailed model of the cone response that incorporated light adaptation and parameters of the rod phototransduction cascade. The van Hateren model used first-order filters with two stages of divisive feedback, derived from calcium feedback in the outer segment and conductance changes in the inner segment. The model was developed to fit our previously published data from macaque H1 horizontal cells (Lee, Dacey, Smith, & Pokorny, 2003; Smith et al., 2001). Since we are concerned only with the linear sinusoidal approach, the quasi-linear model (Smith et al., 2001) using low-pass filters and free scaling is adequate and proved sufficient. For fitting of the RGC data we allowed parallel cascades for center and surround. These were then combined by vector summation allowing a fixed phase offset of π radians. An example of this approach was given by Frishman, Freeman, Troy, Schweitzer-Tong, and Enroth-Cugell (1987) who modeled the spatiotemporal CSF of the cat.

3. Results

3.1. Temporal response and adaptation of H1 cells

We first consider the temporal response of the H1 cell as a function of retinal illuminance, and show that a characteristic 40 Hz resonance in the H1 cell response is likely to reside in the horizontal cell syncytium and thus need not be considered when analyzing ganglion cell responses.

Data for an individual H1 cell are shown at three retinal illuminances in Fig. 1a. The upper panel shows amplitude sensitivity plotted against temporal frequency in a double logarithmic plot. The lower panel shows the response phase. The amplitude characteristic is primarily low-pass, with a slight low frequency roll-off below 5 Hz. At low frequencies, amplitude sensitivity decreased as retinal illuminance increased. The maximum change was 1.5 log unit compared with the 2 log units required by a gain mechanism obeying Weber's Law. At high frequencies the data from different retinal illuminances converge. The phase delay increased by about one radian at 10 Hz as retinal illuminance was decreased. The data showed a pronounced resonant shoulder near 40 Hz. We obtained such data on a sample of 7 cells. The major inter-cell variation was in the sensitivity and in the amplitude and position of the resonance peak. As a result of the latter variation an average could not be fit well with the linear systems model. Examples of other cells were shown previously (Smith et al., 2001).

The solid lines are the fits of the linear systems model, detailed in Smith et al. (2001) and shown as a block diagram in Fig. 2a. The model needed a total of seven stages of first order filter: three stages with a time constant of 2 ms, one stage whose time constant varied with retinal illuminance, and three stages with a fixed time constant near 4 ms. The modest low frequency roll-off was described by a lead-lag filter with a time constant of 2.0 s and a weight α of 1.5. These parameters gave a roll-off of 0.18 log unit that became evident below 5 Hz. There was a second order filter with resonant frequency near 35 Hz and a variable damping constant. The second order filter frequency $(1000/(2\pi\tau_2)$ was fixed by the time constant of the three-stage filter to reduce the number of free parameters.

In summary the variable parameters included: (1) the illuminance-dependant time constant, τ_1 of the one-stage filter, (2) the time constant, τ_2 of the three-stage filter, (3) the value, ζ of the damping constant, and (4) a scaling constant at each illuminance. The four parameters were allowed to vary at each illuminance level. The estimated parameters are summarized in Table 1. As retinal illuminance was reduced, the time constant, τ_1 of the one-stage filter lengthened, approximately tripling with each decade of luminance decrease. The other parameters changed only in a minor way.

We previously suggested that the resonance phenomenon originated in the H1 cell syncytium. The size of the damping phenomenon did not depend on luminance or contrast but did show a strong dependence on test field area. To investigate this phenomenon further, we obtained temporal frequency data using carbenoxolone to block gap junctions (Kamermans & Fahrenfort, 2004; Vaney, Nelson, & Pow, 1998). These data were obtained in conjunction with a study of the H1 cell receptive field and the methods are described elsewhere (Packer & Dacey, 2002). Briefly, the pre-carbenoxolone TCSF was measured at c. 50 td at a fixed contrast of 0.5. The drug (100 mmol) was applied to the perfusion drip and the change in membrane potential was monitored using a continuous 2 Hz square wave. The membrane hyperpolarized, reducing the size of the 2 Hz response. After the response stabilized (c. 10 min), the TCSF was remeasured. The drug was removed and membrane potential was monitored as above until recovery was obtained (c. 20 min) and a final post-carbenoxolone TCSF was obtained. Five cells were investigated. The data from one cell are shown in Fig. 1b as amplitude sensitivity and phase plotted vs. frequency. The TCSF measured under carbenoxolone showed an overall reduction in sensitivity (about 0.3 log unit and loss of the resonance peak. The solid lines show simultaneous fits of the linear systems model to all three data sets. For the carbenoxolone data, only the damping constant and the amplitude scaling factor were

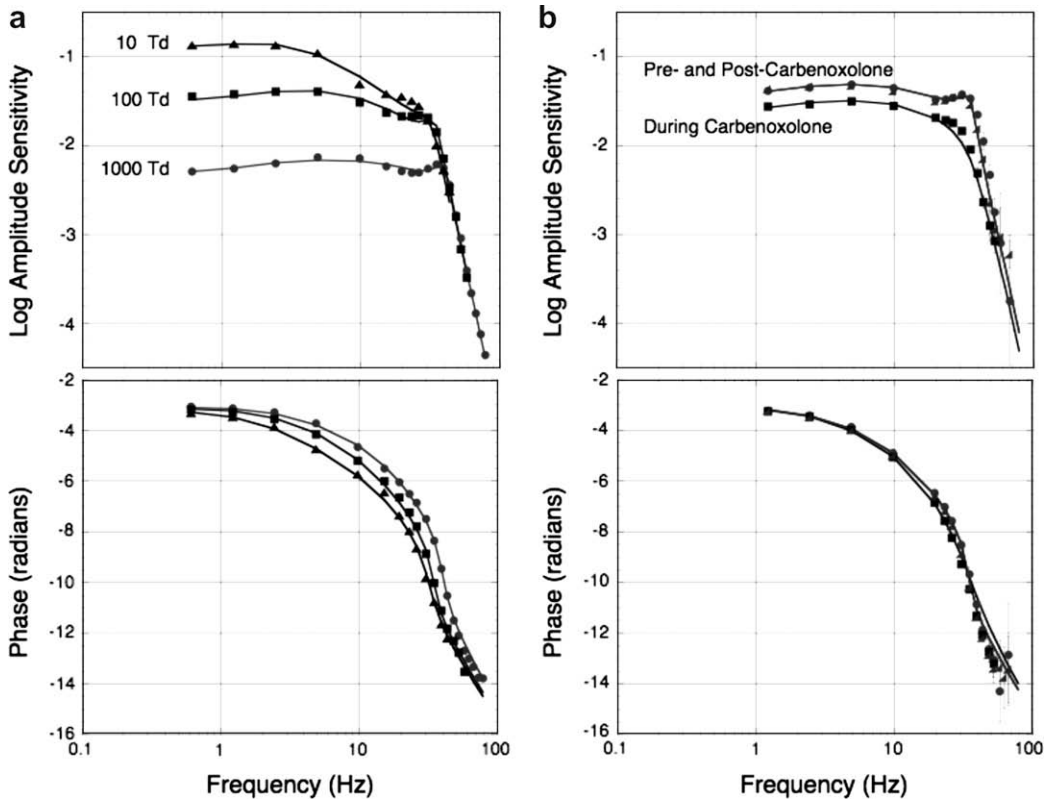

Fig. 1. (a) Log amplitude sensitivity (mV/*C*/illuminance) and phase (radians) as a function of temporal frequency and average retinal illumination level. Data are from an H1 cell. The lines are fits of a linear systems model described in the text. (b) The effect of carbenoxolone on the temporal amplitude sensitivity of an H1 cell.

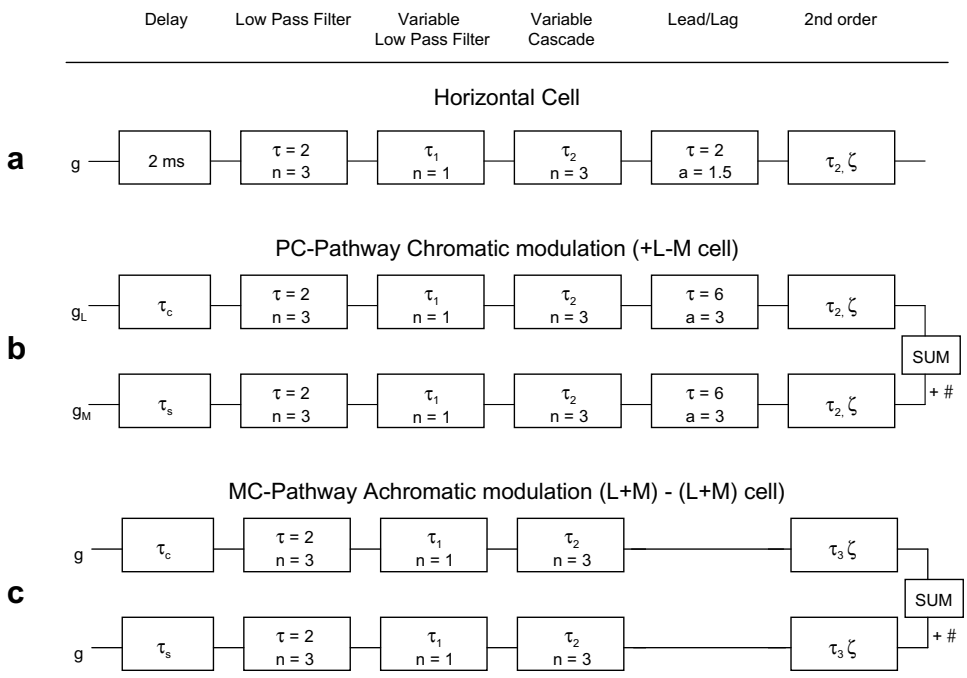

Fig. 2. (a) Diagram of the linear cascade used to model the H1 cell. (b) Diagram of the linear cascade used to model the PC-cell. This diagram shows an (L–M) cell response to chromatic modulation. (c) Diagram of the linear cascade used to model the MC-cell.

Table 1
Model fit parameters for the H1 cell, PC-pathway cell, MC-pathway cell and human response temporal contrast sensitivity functions

Element	Stage	Retinal illuminance (Td)						
		2	10	20	100	200	1000	2000
H1 cell fit parameters								
1st order	One stage	–	45	–	14	–	4	–
1st order	Three stage	–	5	–	4.6	–	4	–
2nd order		–	–	–	–	–	–	–
	ζ	–	1.5	–	0.05	–	0.5	–
PC-pathway cell fit parameters								
1st order	One stage	–	–	16	–	7	–	4
1st order	Three stage	–	–	4.5	–	4	–	3
Center delay		–	–	9.5	–	9.5	–	9.5
Surround delay		–	–	4.5	–	4.5	–	4.5
MC-pathway cell fit parameters								
1st order	One stage	43	–	22	–	6.5	–	2.4
1st order	Three stage	43	–	22	–	6.5	–	2.4
Center delay		6.6	–	6.6	–	6.6	–	6.6
Surround delay		9.0	–	9	–	9	–	9
Human response								
Achromatic MC+	Four stage	11.5	–	11.5	–	11.5	–	11.5
Chromatic PC+	Four stage	31.2	–	31.2	–	31.2	–	31.2

allowed to vary. The model provides an adequate description of the data and confirms the previous conclusion that the resonance arises from the input from lateral connections from other H1 cells in the syncytium to the H1 cell.

3.2. Adaptation and temporal response of PC-pathway cells resembles outer retina

We now consider the temporal response of the PC-cell and show combination of opponent cone signals with the temporal characteristics of the horizontal cells could well account for the responses.

Data for PC-pathway cells ($n = 25$) with chromatic modulation are shown in Fig. 3a for a range of retinal illuminance from 20 to 2000 td. The PC-cells TCSFs primarily varied in sensitivity, allowing us to average the responsivity functions. We averaged at least 5–10 cells per condition, though data were not obtained for all cells at all retinal illuminances (Lee et al., 1990). In particular, only minimal data for a few cells could be obtained at 2 td and some of those gave evidence of rod intrusion. We have omitted this data set. The functions were primarily low-pass but there was an obvious low frequency roll-off below 10 Hz. The high frequency cut-off was similar to the H1 cell data. The reduction in amplitude sensitivity with luminance was about 1.5 log unit between 20 and 2000 td, similar to the H1 cell data. The phase delay similarly increased by about one radian at 10 Hz as retinal illuminance was decreased.

The solid lines are the fits of the model outlined in Fig. 2b. For PC-cells we allow two parallel sets of filters for center and sur-

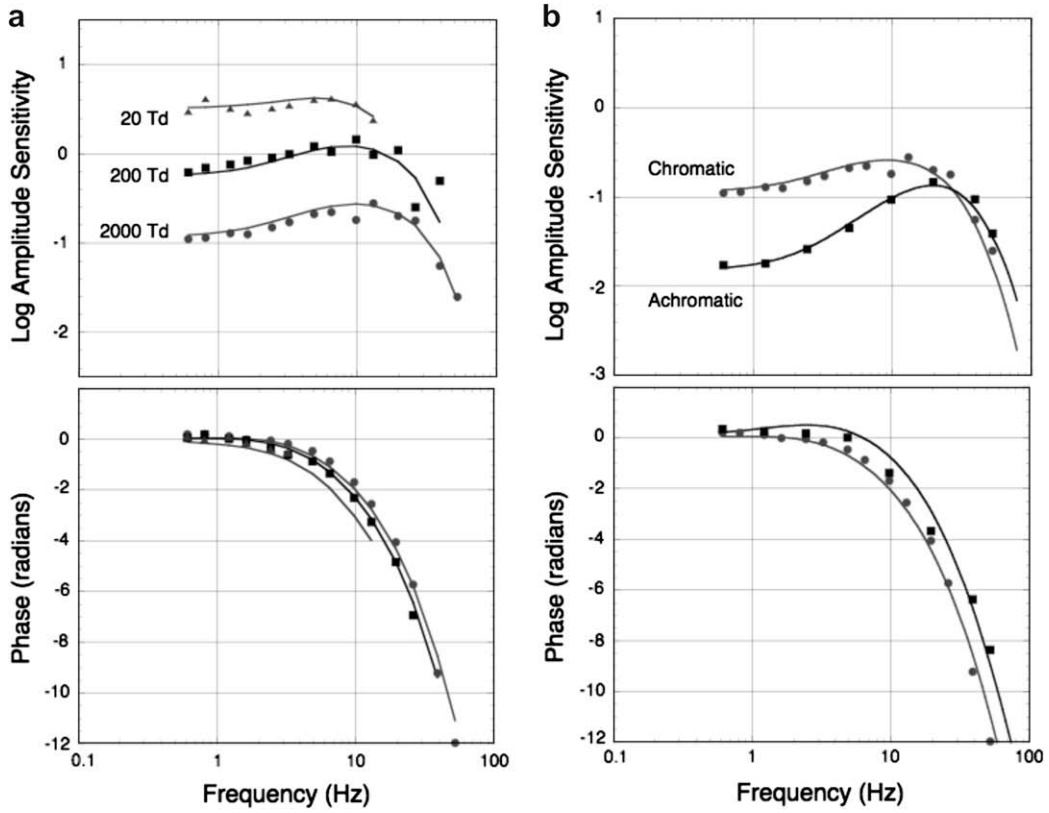

Fig. 3. PC cells: (a) Log chromatic amplitude sensitivity (R_{max}/C_{sat}/illuminance) and phase (radians) as a function of temporal frequency and average retinal illumination level. The lines are fits of a linear systems model described in the text. (b) Comparison of chromatic and achromatic data at 2000 td.

round, using the same filter cascade shown in Fig. 2a. The surround is given a phase delay of π. Fig. 2b shows the example for a +L–M cell and chromatic modulation. We associate the L cone response with the center and the M cone response with the surround. For chromatic modulation the lights are out of phase. We calculated phase data relative to the 638 nm LED. A phase factor of π radians is added to the surround M cone phase. The second order filter was used but based on the data of Fig. 3a, we fixed the damping constant, ζ to 1. At this value the second order filter reduces to a cascade of two first order filters with a time constant, τ_2. The more pronounced low frequency roll-off was described by a lead-lag filter with a time constant of 6.0 s and a weight α of 3. These parameters gave a roll-off of 0.48 log unit that became evident below 10 Hz. The center–surround response was calculated by vector addition, allowing a center–surround weight and a center–surround delay, which were constant with retinal illuminance. We calculated relative chromatic and achromatic sensitivity factors based on the LED calibrations and the Smith–Pokorny fundamentals. To simplify the fits, the overall gain of the center was determined by a function relating output to illuminance. This function was the form of a gain function entering at 3 td with a power of 0.7. It was designed to mimic the degree of light adaptation observed in H1 cells. These factors were used to weight the center and surround gains and only one scaling factor was needed for all three luminance levels.

For the PC-cells the variable parameters included: (1) the time constant, τ_1 of the one-stage filter, (2) the time constant, τ_2 of the three-stage filter, (3) the fixed delays, τ_C, τ_S of the center and surround, (4) the center/surround ratio and a scaling constant at each illuminance. The time constants were allowed to vary across illuminance level; the delays and scaling constant were fixed. Simultaneous fits were established for chromatic modulation at all three levels and achromatic modulation at 2000 td. The temporal parameters are summarized in Table 1. As retinal illuminance was reduced, the time constant, τ_1 of the one-stage filter lengthened, approximately tripling with each decade of luminance decrease. The other parameters changed little.

Good fits were obtained using similar time constants for the first order filters as for the H1 cell (Table 1). The center–surround delay was 4 ms, which was within the range of values obtained for PC cells in an independent analysis (Smith et al., 1992). Fig. 3b shows data comparing chromatic and achromatic modulation at 2000 td. For achromatic modulation, the cones are in phase and the ≠ phase delay added to the M cone in Fig. 2b is removed. The TCSF is band-pass since the PC-cell now shows center–surround subtraction. The intersection of the chromatic and achromatic TCSFs is determined by the center–surround delay and the center–surround weighting. The model describes this feature adequately.

In conclusion, for the midget system, our data suggest that the temporal dynamics and the amount of adaptation changed little between photoreceptor and midget retinal ganglion cell.

3.3. MC-pathway cells show additional gain controls and temporal filtering

We now consider the temporal response of the MC-cell and demonstrate that to describe these cells' responses additional, presumably inner retinal, gain controls are required.

Responsivity data for MC-pathway cells ($n = 27$) with achromatic modulation are shown in Fig. 4 for a range of retinal illuminance from 2 to 2000 td. These data represent an average of at least 5–10 cells per illumination level, but data were not obtained for all cells at all retinal illuminances (Lee et al., 1990). The functions

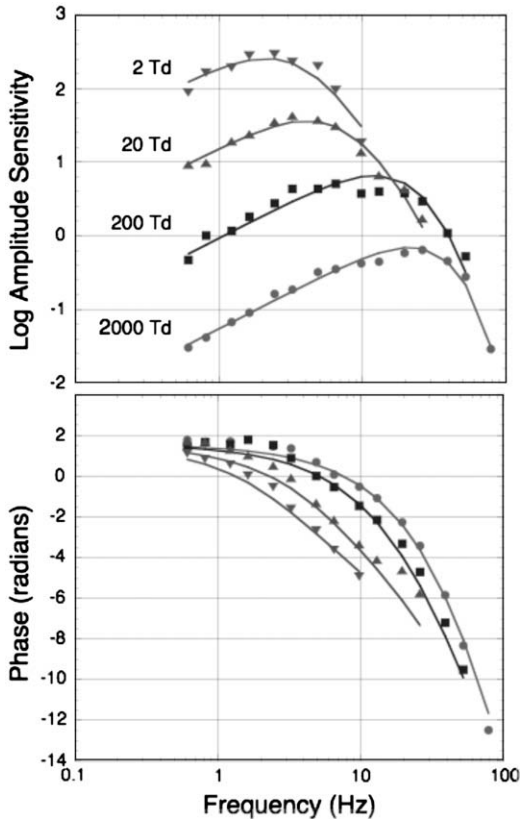

Fig. 4. MC-cells: Log amplitude sensitivity (R_{max}/C_{sat}/illuminance) and phase (radians) as a function of temporal frequency and average retinal illumination level. The lines are fits of a linear systems model described in the text.

were primarily band-pass, and the peak sensitivity was displaced to lower temporal frequencies as retinal illuminance was decreased. The high frequency cut-off was similar to or higher than the H1 cell data. The reduction in amplitude sensitivity with luminance was over 3 log unit between 2 and 2000 td, consistent with Weber's law. The phase of response showed a phase advance of $\pi/2$ at low frequencies, a characteristic of transiency and center–surround subtraction. There were phase delays of 4 radians at 10 Hz as retinal illuminance was decreased.

The separation of the TCSFs was greater than a log unit per decade at low frequencies. Lee et al. (1990) ascribed this to greater surround strength at high retinal illuminances; a set of data with small spot stimuli showed more precise Weber behavior (not shown). At high illuminance, the MC-pathway cell response was 8- to 9-fold more sensitive than the PC-pathway response to achromatic stimulation at its peak.

The shift in peak sensitivity and the greater illuminance dependence of the phase data suggested additional illuminance-dependent changes in the time constants subsequent to the H1 cell. The solid lines are the fits of the linear systems model outlined in Fig. 2c. As for PC-cells we allowed two parallel sets of filters for center and surround, using the same filter cascades shown in Fig. 2a. The surround was given a delay of π. The second order filter was used but again we set the damping constant, ζ to 1. In the MC-cell, the pronounced roll-off is due to center–surround subtraction and the lead-lag filter did not prove useful. The center–surround weight was set at unity to give the 90° phase advance at low frequencies. In pilot runs, we found we could obtain good solutions with the second order filter frequency fixed at 50 Hz ($\tau = 3.18$).

For the MC-cells the variable parameters included: (1) the time constant, τ_1 of the one-stage filter, (2) the time constant, τ_2 of the three-stage filter, (3) the fixed delays, τ_C, τ_S of the center and surround, (4) the gain g_C of the center. The time constants and gain were allowed to vary across illuminance level; the delays were fixed. Again, the center–surround response was calculated by vector addition.

We found that good fits were obtained when both time constants, τ_1 and τ_2, increased as illumination decreased (Table 1). The change was an approximate doubling for each decade decrease in illuminance. We conclude that in the MC system there is evidence of additional gain control beyond the photoreceptor. The system is one in which the gain and the time constant are linked. Increased sensitivity at low retinal illuminances is achieved at the cost of a decrease in temporal resolution (Donner & Hemila, 1996). A recent study of photoreceptor, bipolar and retinal ganglion cells (Dunn, Lankheet, & Rieke, 2007) also proposed two sites of adaptation, one in the cone photoreceptors and one at the bipolar–retinal ganglion cell junction. This study however did not involve analysis of the temporal parameters and did not distinguish between adaptation in the PC midget vs the MC parasol pathway.

4. Discussion

We have shown that it is possible to trace the temporal contrast sensitivity function through the retina using a quasi-linear systems approach and limited constraints. Linear systems approaches are subject to the criticism that neuronal responses show significant nonlinearities. To avoid this difficulty, we used responsivity measures where responses are small and neurons are likely to operate in a linear range. Cat retinal ganglion cell data are also well described by a linear systems approach with similar elements (Frishman et al., 1987). We have found that our model also describes individual ganglion cell's responsivity data; we achieve good fits for measurements at all contrasts for PC-pathway cells, but good fits are restricted to low contrast for MC-pathway cells. The fit parameters agree with the average data summarized in Table 1. Individual cells varied primarily in sensitivity and only slightly in time constants.

We also found that it was not necessary to allow the center–surround delays or the center–surround weights to vary with retinal illuminance. In initial fits we allowed such variation but this did not improve the fits.

The final step, the link from the retinal ganglion cells to visual psychophysics, was first suggested by Lee et al. (1990) and further emphasized in subsequent publications (Kremers, Lee, Pokorny, & Smith, 1993; Yeh, Lee, & Kremers, 1995). For chromatic modulation, temporal contrast sensitivity functions of PC-pathway cells and psychophysical data both show a low-pass shape that decreases in contrast sensitivity as retinal illuminance is increased, i.e., Weber's Law is not evident in either data set. The shape of the temporal contrast sensitivity functions is very similar for MC-pathway cells and psychophysical data using luminance contrast. Both show a transition from low-pass to band-pass shape as retinal illuminance is increased. Weber's Law is evident at the level of the retinal ganglion cell. The major distinctions between physiology and psychophysics are the losses of high frequency resolution in the psychophysical data.

Chromatic temporal resolution is good in the PC-pathway but very poor in visual psychophysics. This loss of temporal resolution makes possible the use of heterochromatic flicker photometry to match luminance of different spectral lights. Fig. 5 (upper panel) shows psychophysical chromatic temporal sensitivity data of Swanson et al. (1987) measured in the fovea. The lines show fits obtained by taking the PC-cell predictions, and adding further low-pass filtering. We used a four-stage 31.2 ms linear filter.

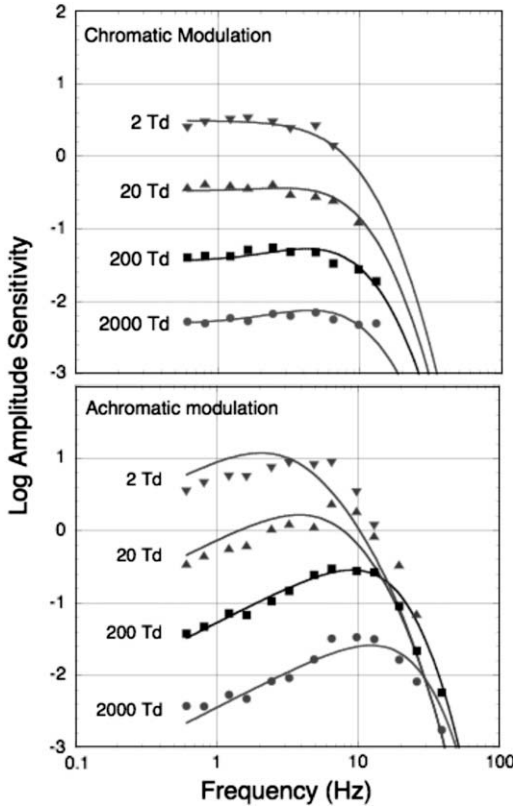

Fig. 5. Psychophysics: Log amplitude sensitivity ($1/C_{th}$/illumination). C_{th} is the contrast for a threshold percept of flicker. Upper panel shows chromatic sensitivity; lower panel shows achromatic sensitivity.

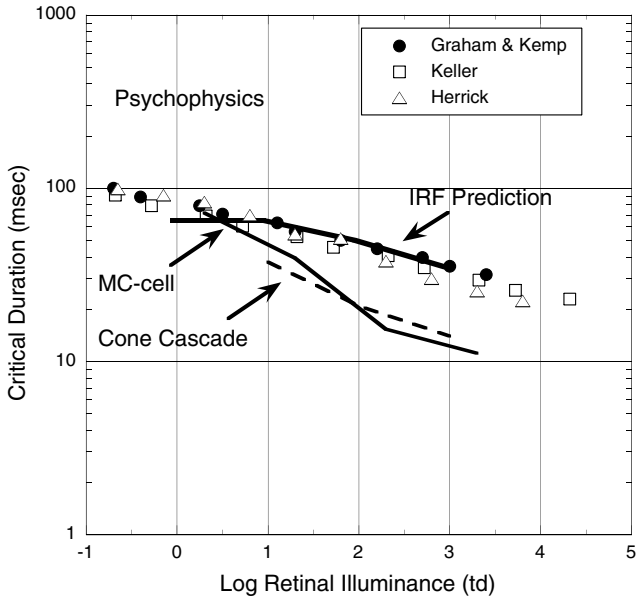

Fig. 6. Critical duration as a function of illuminance level. The data points are data from three classical psychophysical studies. The solid and dashed lines are calculations from the models presented in Figs. 1, 4 and 5.

We allowed individual scaling and this showed a systematic change in sensitivity with a range of 0.8 log unit per log unit of illuminance change. It appears that the PC-pathway gives up temporal resolution, presumably to allow temporal pooling of its signals in the visual cortex.

The difference in temporal resolution of the MC-pathway cells and psychophysics is less pronounced. Observers can resolve temporal modulations as high as 80 Hz under optimal conditions (Tyler & Hamer, 1990). Fig. 5 (lower panel) shows psychophysical achromatic temporal sensitivity data of Swanson et al. (1987) measured at the fovea. The lines show fits obtained by taking the MC-cell predictions and adding further low-pass filtering. We used a four-stage 11.56 ms linear filter. This filter may represent a feature of ganglion cell output rather than a post-retinal filter *per se*. A neurometric approach has recently shown that cell responses become variable at high frequencies as a consequence of impulse statistics, and little filtering of the MC-pathway is required (Lee, Sun, & Zucchini, 2007). This suggests that low-pass filtering by the visual cortex reduces the temporal resolution of the MC-pathway only modestly if at all.

One advantage of the linear modeling approach is that we can equally work in the time domain, allowing us to examine the effect of pulse duration on visual thresholds for discrete stimuli. For very short exposure durations there is complete temporal summation and thresholds depend on total energy, the product of luminous flux and time. For longer exposure times, energy increases with exposure duration and is dependent solely on luminous flux. The critical duration is the pulse duration at the transition between these two regions. Critical duration varies as a function of the retinal illumination of an adapting field. In human psychophysics critical duration decreases from about 100 ms at cone threshold to 20 ms at 10,000 td. Data of Graham and Kemp (1938), Herrick (1956) and Keller (1941) are shown in Fig. 6. The three lines represent model predictions of critical duration at the cone level (measured in H1 cells), at the magnocellular cell level, and the psychophysical level.

In conclusion, we suggest that sensitivity regulation in the primate retina involves multiple time-dependent mechanisms. An early stage of adaptation in the outer retina is common to both PC- and MC-pathways. The MC-pathway then trades temporal processing for sensitivity to increase responsivity at low photopic light levels. This mechanism appears to occur at the ganglion cell level (Dunn et al., 2007), and produces Weber's Law. The PC-pathway trades temporal resolution for sensitivity at all photopic levels through a cortical mechanism. The long time constant increases the signal-to-noise ratio and may improve sensitivity to stable chromatic and achromatic contrast.

Acknowledgments

NIH, UPHS grants EY00901 (JP), EY13112 (BBL) and EY09625 (DMD), and a Research to Prevent Blindness Challenge Grant supported this work. We thank Orin Packer for collecting the H1 carbenoxolone data.

References

Boycott, B. B., & Dowling, J. E. (1969). Organization of the primate retina: Light microscopy. *Philosophical Transactions of the Royal Society of London B, 255*, 109–184.

Boycott, B. B., & Kolb, H. (1973). The horizontal cells of the rhesus monkey retina. *Journal of Comparative Neurology, 148*, 91–114.

Dacey, D. M., Diller, L. C., Verweij, J., & Williams, D. R. (2000). Physiology of L- and M-cone inputs to H1 horizontal cells in the primate retina. *Journal of the Optical Society A, 17*, 589–596.

Dacey, D. M., Lee, B. B., Stafford, D. K., Pokorny, J., & Smith, V. C. (1996). Horizontal cells of the primate retina: Cone specificity without spectral opponency. *Science, 271*, 656–659.

de Lange, H. (1954). Experiments on flicker and some calculations on an electrical analogue of the foveal systems. *Physica, 8*, 935–950.

de Lange, H. (1958). Research into the dynamic nature of the human fovea-cortex systems with intermittent and modulated light. I. Attenuation characteristics with white and colored light. *Journal of the Optical Society of America, 48*, 777–784.

Donner, K., & Hemila, S. (1996). Modelling the spatio-temporal modulation response of ganglion cells with difference-of-Gaussians receptive fields: Relation to photoreceptor response kinetics. *Visual Neuroscience, 13*, 173–186.

Dunn, F. A., Lankheet, M. J., & Rieke, F. (2007). Light adaptation in cone vision involves switching between receptor and post-receptor sites. *Nature, 449*, 603–606.

Frishman, L. J., Freeman, A. W., Troy, J. B., Schweitzer-Tong, D. E., & Enroth-Cugell, C. (1987). Spatiotemporal frequency responses of cat retinal ganglion cells. *Journal of General Physiology, 89*, 599–628.

Goodchild, A. K., Chan, T. L., & Grunert, U. (1996). Horizontal cell connections with short-wavelength-sensitive cones in macaque monkey retina. *Visual Neuroscience, 13*(5), 833–845.

Graham, C. H., & Kemp, E. H. (1938). Brightness discrimination as a function of the increment in intensity. *Journal of General Physiology, 21*, 635–650.

Herrick, R. M. (1956). Foveal luminance discrimination as a function of the duration of the decrement or increment in luminance. *Journal of Comparative and Physiological Psychology, 49*, 437–443.

Hood, D. C., & Birch, D. G. (1993). Human cone receptor activity: The leading edge of the a-wave and models of receptor activity. *Visual Neuroscience, 10*, 857–871.

Kamermans, M., & Fahrenfort, I. (2004). Ephaptic interactions within a chemical synapse: Hemichannel-mediated ephaptic inhibition in the retina. *Current Opinion in Neurobiology, 14*, 531–541.

Keller, M. (1941). The relation between the critical duration and intensity in brightness discrimination. *Journal of Experimental Psychology, 28*, 407–418.

Kelly, D. H. (1961). Visual responses to time-dependent stimuli: I. Amplitude sensitivity measurements. *Journal of the Optical Society of America, 51*, 422–429.

Kelly, D. H. (1974). Spatio-temporal frequency characteristics of color-vision mechanisms. *Journal of the Optical Society of America, 64*, 983–990.

Kremers, J., Lee, B. B., Pokorny, J., & Smith, V. C. (1993). Responses of macaque ganglion cells and human observers to compound periodic waveforms. *Vision Research, 33*, 1997–2011.

Lamb, T. D., & Pugh, E. N. J. (1992). A quantitative account of the activation steps involved in phototransduction in amphibian photoreceptors. *Journal of Physiology, 449*, 719–758.

Lee, B. B., Dacey, D. M., Smith, V. C., & Pokorny, J. (2003). Dynamics of sensitivity regulation in primate outer retina: The horizontal cell network. *Journal of Vision, 3*, 513–526. http://journalofvision.org/3/7/5/.

Lee, B. B., Martin, P. R., & Valberg, A. (1989). Sensitivity of macaque retinal ganglion cells to chromatic and luminance flicker. *Journal of Physiology (London), 414*, 223–243.

Lee, B. B., Pokorny, J., Smith, V. C., Martin, P. R., & Valberg, A. (1990). Luminance and chromatic modulation sensitivity of macaque ganglion cells and human observers. *Journal of the Optical Society of America A, 7*, 2223–2236.

Lee, B. B., Sun, H., & Zucchini, W. (2007). The temporal response of macaque ganglion cells and central mechanisms of flicker detection. *Journal of Vision, 7*, 1–16.

Milsum, J. H. (1966). *Biological control systems analysis*. New York: McGraw-Hill.

Packer, O. S., & Dacey, D. M. (2002). Receptive field structure of H1 horizontal cells in macaque monkey retina. *Journal of Vision, 2*, 272–292.

Smith, V. C., Lee, B. B., Pokorny, J., Martin, P. R., & Valberg, A. (1992). Responses of macaque ganglion cells to the relative phase of heterochromatically modulated lights. *Journal of Physiology (London), 458*, 191–221.

Smith, V. C., Pokorny, J., Lee, B. B., & Dacey, D. M. (2001). Primate horizontal cell dynamics: An analysis of sensitivity regulation in the outer retina. *Journal of Neurophysiology, 85*, 545–558.

Solomon, S. G., Martin, P. R., White, A. J., Ruttiger, L., & Lee, B. B. (2002). Modulation sensitivity of ganglion cells in peripheral retina of macaque. *Vision Research, 42*, 2893–2898.

Swanson, W. H., Ueno, T., Smith, V. C., & Pokorny, J. (1987). Temporal modulation sensitivity and pulse detection thresholds for chromatic and luminance perturbations. *Journal of the Optical Society of America A, 4*, 1992–2005.

Tyler, C. W., & Hamer, R. D. (1990). Analysis of visual modulation sensitivity. IV. Validity of the Ferry–Porter law. *Journal of the Optical Society of America A, 7*, 743–758.

van Hateren, J. H. (2005). A cellular and molecular model of response kinetics and adaptation in primate cones and horizontal cells. *Journal of Vision, 5*, 331–347. http://journalofvision.org/335/334/335/.

van Hateren, J. H. (2007). A model of spatiotemporal signal processing by primate cones and horizontal cells. *Journal of Vision, 7*(3), 1–19. http://journalofvision.org/17/13/13/.

Vaney, D. I., Nelson, J. C., & Pow, D. V. (1998). Neurotransmitter coupling through gap junctions in the retina. *Journal of Neuroscience, 18*, 10594–10602.

Verweij, J., Peterson, B. B., Dacey, D. M., & Buck, S. L. (1999). Sensitivity and dynamics of rod signals in H1 horizontal cells of the macaque monkey retina. *Vision Research, 39*, 3662–3672.

Yeh, T., Lee, B. B., & Kremers, J. (1995). The temporal response of ganglion cells of the macaque retina to cone-specific modulation. *Journal of the Optical Society of America A, 12*, 456–464.